Journal of Power Sources 214 (2012) 28–32

Contents lists available at SciVerse ScienceDirect

Journal of Power Sources

journal homepage: www.elsevier.com/locate/jpowsour

Short communication

Experimental and simulated investigation of 1 kW solid oxide fuel cell balance of power system

Sung Kook Hong*, Sang Keun Dong, Je Bok Yang

Energy Efficiency Department, Korea Institute of Energy Research, 152, Gajeong-ro, Yuseong-gu, Dajeon 305-343, Republic of Korea

ARTICLE INFO

Article history:
Received 9 February 2012
Received in revised form
3 April 2012
Accepted 6 April 2012
Available online 25 April 2012

Keywords:
Solid oxide fuel cell (SOFC)
Balance of power (BOP)
Autothermal reformer
Dynamic simulation

ABSTRACT

A 1 kW solid oxide fuel cell (SOFC) balance of power (BOP) system is analyzed using experiments and simulations to optimize the design and operating conditions. The system consists of an autothermal reformer, combined heat exchanger and afterburner, and dummy stack. Thermolib program is used for the simulations.

The system exhibits stable operation during a two cycle on/off experiment. The simulated results obtained by zero-dimensional modeling are similar to the experimental results although a discrepancy appears early in operation owing to the simplified modeling. The system's characteristics are also investigated in terms of the fuel utilization, presence or absence of internal reforming and external heat transfer coefficient.

1. Introduction

Growing concern about the environment has spurred the considerable efforts at developing energy conversion devices for transportation and stationary use. Fuel cells are one option for replacing conventional devices. Among various types of fuel cells, a great number of researchers have investigated the solid oxide fuel cell (SOFC) in the past decades because it offers higher efficiency than other types. SOFCs are expected to be applied to diverse applications such as residential power generator (RPG), auxiliary power unit (APU), and power plant. An SOFC system requires the use of multiple technologies, including a suitable material, stacking, and system integration [1,2].

For optimum SOFC operation, it is important to design an efficient balance of power (BOP) and to achieve high stack performance. Therefore, many studies have investigated SOFC BOP systems [3–6]. In addition to experiments, simulations have been conducted recently because the simulated results can be used to optimize the system configuration, considering transient characteristics.

Lawrence et al. [4] used the Simulink for a 1 kW APU system to examine the heat and mass balance. Lu et al. [5] also used a Simulink model consisting of three main modules, the stack, combustor, and heat exchanger. They estimated the temperature and output voltage response to a sudden load change within the stack. Salogni et al. [6] employed a non-linear dynamic lumped parameters model for an SOFC stack and connected it to additional components and subsystems to evaluate the system characteristics under various operation parameters.

However, few studies have compared the experimental and simulated results [7,8]. Therefore, an SOFC BOP system with integrated components was designed and tested in this study, and the results of dynamic simulation were compared with experimental data in order to evaluate the system.

2. Experimental apparatus

Fig. 1 shows a schematic of the SOFC BOP system within a hot box; the system consists of an autothermal reformer (ATR), combined heat exchanger and afterburner, and dummy stack. The autothermal reformer was designed to use the exhausted gas from the afterburner. The heat exchanger for preheating the reforming reactant and cathode air was integrated with the afterburner (catalytic burner) in order to minimize heat loss and maximize the use of the exhausted heat. A dummy stack consisting of a heat exchanger, including a catalyst, was used to simulate the consumption of the simulated fuel (H_2 and CO) within the stack; Additional air was supplied to the anode side and part of the simulated fuel reacted with the air and was depleted within the anode side.

* Corresponding author. Tel.: +82 42 860 3308; fax: +82 42 860 3102.
E-mail address: sungkookhong@kier.re.kr (S.K. Hong).

0378-7753/$ – see front matter © 2012 Elsevier B.V. All rights reserved.
doi:10.1016/j.jpowsour.2012.04.044

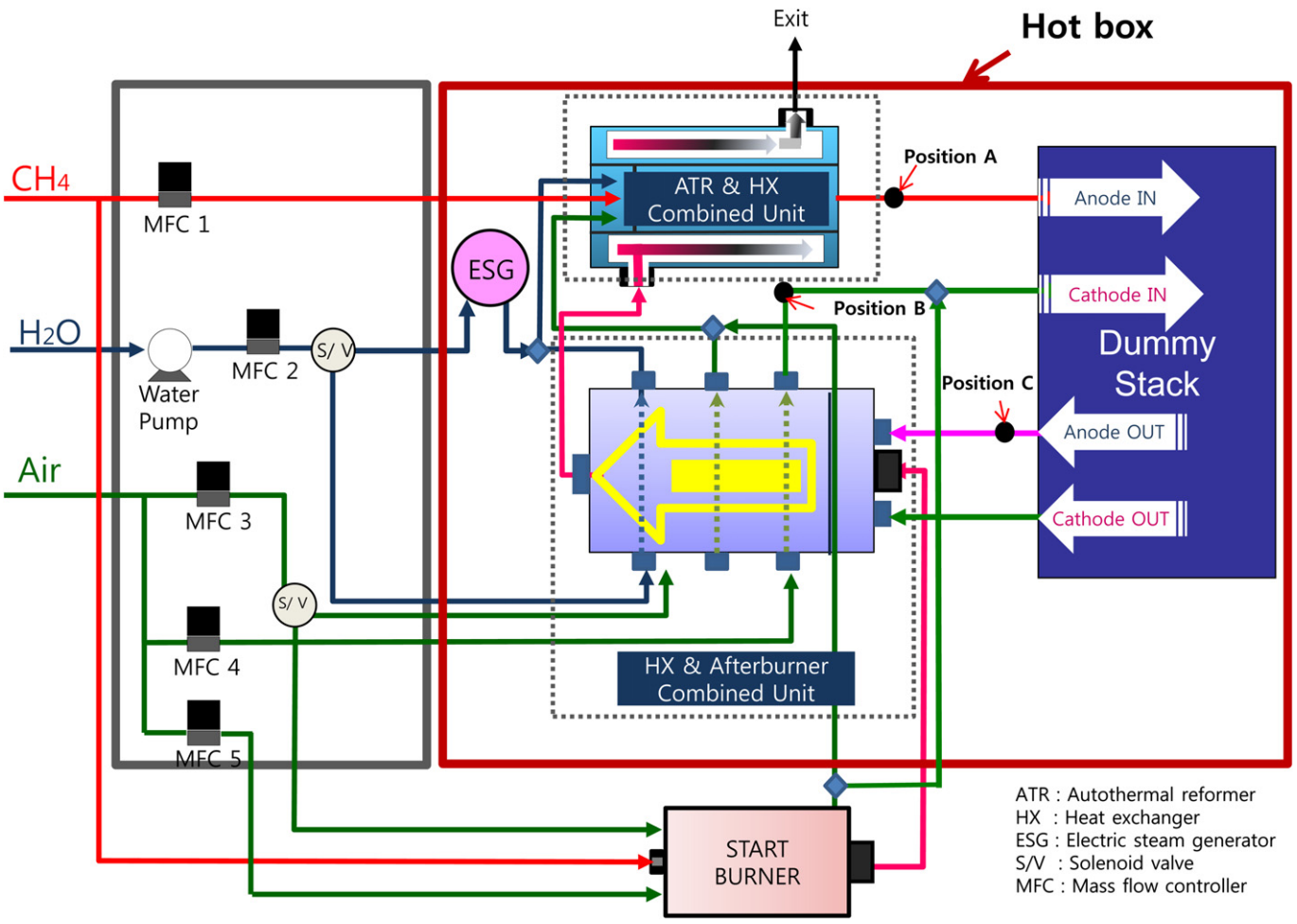

Fig. 1. Schematic of SOFC BOP system.

The SOFC BOP system test rig was set up as shown in Fig. 2. A data acquisition system, control panel, and external start burner were installed next to the hot box. The temperature of gas on each component was measured using K-type thermocouples at position A, B, and C (Fig. 1). A gas analyzer (K1550, Hitech instruments, UK) was connected to the bypass line of the ATR and dummy stack (positions A and C) to analyze the gas.

The system operates as follows; First, the start burner turns on, heating the system. Second, the fuel is supplied to the ATR. Third, the system switches to the independent operation mode after the start burner is turned off. A two cycle on/off experiment was performed using this scenario. When the system reaches the steady state, fuel injection shuts down for 7 h, and then the same operating process occurs again.

For reforming, CH_4 (0.38 Nm^3hr^{-1}) was injected into the ATR with the steam and air. The steam to carbon ratio (SCR) and oxygen to carbon ratio (OCR) were fixed at 1.12 and 0.88, respectively; these values were determined in a previous study [9].

3. Simulation set up

Thermolib (Release 4.2), which is based on MATLAB, was used to model the SOFC BOP system [10]. The simulation program employed the zero-dimensional model, which is the simplest one considering mass and energy balance.

The simulation model consisted of several modules including a heat exchanger, reactor, burner, three-way valve, and user-subsystem. For ATR modeling, a chemical equilibrium considering the following reactions was used.

$$CH_4 + H_2O \Leftrightarrow CO + 3H_2 \quad (1)$$

$$CH_4 + 1/2O_2 \Leftrightarrow CO + 2H_2 \quad (2)$$

$$H_2O + CO \Leftrightarrow CO_2 + H_2 \quad (3)$$

These reactions were specified to reach thermodynamic equilibrium for a given composition and temperature at a given pressure.

Because the remaining simulated fuel from the stack reacts completely with oxygen in the afterburner, a burner module was selected to simulate complete combustion. The remaining H_2, CO, and CH_4 in the simulated fuel are completely converted to CO_2 and H_2O in the burner module.

$$CH_4 + 2O_2 \Rightarrow CO_2 + 2H_2O \quad (4)$$

$$H_2 + 1/2O_2 \Rightarrow H_2O \quad (5)$$

$$CO + 1/2O_2 \Rightarrow CO_2 \quad (6)$$

In the dummy stack, the above reactions were used to simulate the consumption of the simulated fuel. Meanwhile, in the real stack,

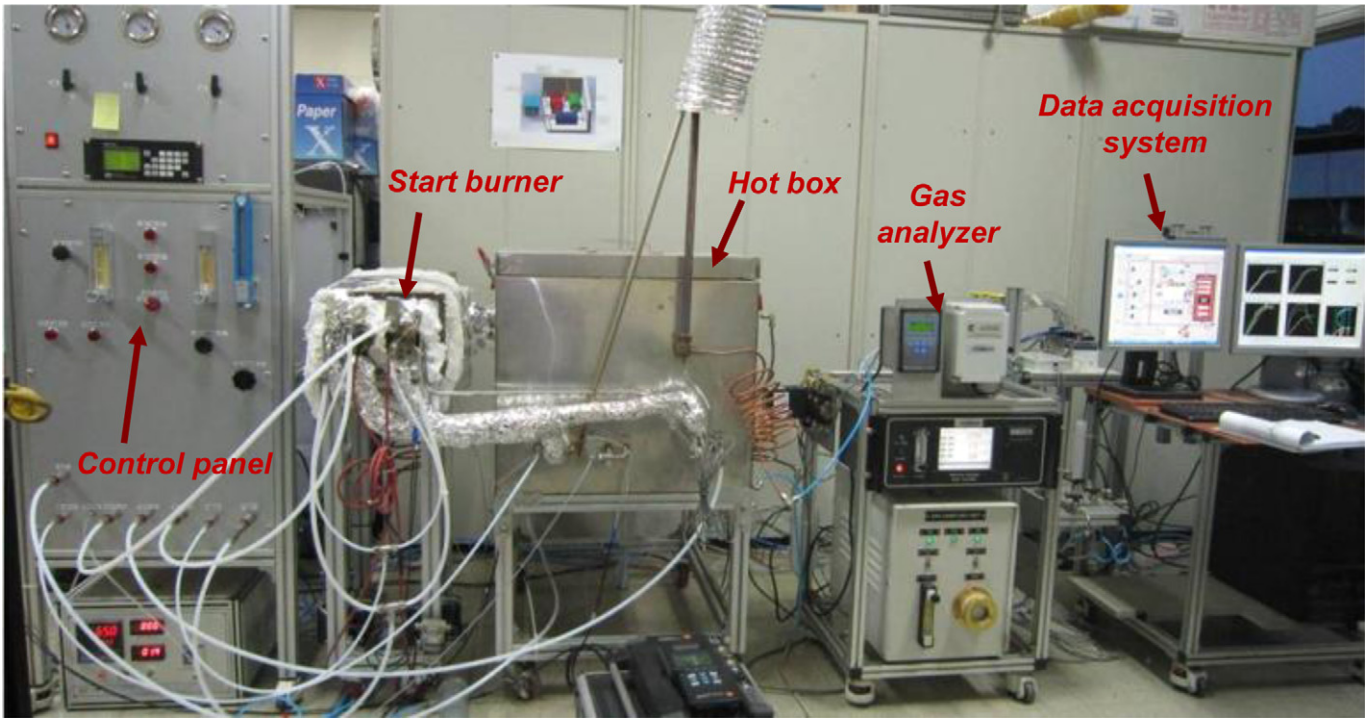

Fig. 2. Test rig of SOFC BOP system.

the electrical power was calculated using amount of available H_2, fuel utilization, and typical I–V curve, and the depletion of fuel in the stack was simulated.

A heat exchanger module considering an effective-NTU method was employed to model the heat exchange process in each component. For the effective-NTU calculation, the heat transfer coefficient at each component was calculated using a convection correlation [11]; The dummy stack and combined heat exchanger are a plate fin type exchanger, and ATR has the configuration of circular tube. The following convection correlations were chosen with respect to the laminar and turbulent flow regimes, respectively.

$$Nu_D = 3.66 \text{ for laminar flow} \quad (7)$$

$$Nu_D = 0.023\, Re_D^{4/5}\, Pr^n \text{ for turbulent flow} \quad (8)$$

For the dynamic analysis, the thermal mass of each component was estimated using its weight. All components were related dynamically to satisfy the mass and energy balance. The values used for each component in the heat exchange calculation are listed in Table 1. The operating scenario is the same as that in the experiment.

4. Results and discussion

Fig. 3 shows the history of the temperature and composition of the gas obtained in the two cycle on/off experiment at positions A, B, and C. The temperature of the gas at each component increased to 600–650 °C and a similar temperature history appeared during both operating cycles, as shown in Fig. 3(a). Start-up required approximately 260 min, although the time required could be changed depending on the start burner's operating conditions.

Table 1
Calculation parameters for heat exchange.

	ATR	Dummy stack	Combined heat exchanger
Surface area (m^2)	0.2	0.2	0.8
Overall heat transfer coefficient ($Wm^{-2}\,K^{-1}$)	30	40	50
Thermal mass ($kJ\,K^{-1}$)	20	9.2	18.4

Fig. 3(b) shows the composition of the gas exiting from the ATR based on the dry condition. Gas reformation occurred immediately after the fuel injection at 140 min. As the temperature within the ATR increased, the amounts of H_2 and CO increased and that of CO_2 decreased owing to increased excitation of the reforming reaction [12]. After 300 min, the ratio of the components became constant. This pattern also appeared in the second cycle experiment, indicating that the ATR produces stable reforming performance.

Fig. 4 compares the experimental and simulated data for the temperature of the cathode air from the heat exchanger (position B) and the composition of the reforming gas from the ATR (position A). As shown in Fig. 4(a), sudden changes in temperature occur at 140 and 260 min, which correspond to the beginning of fuel injection and shutoff of the start burner, respectively. Fig. 4(b) indicates the occurrence of fuel reformation at 140 min and a constant composition of reforming gas after 300 min. The temperature and gas composition estimated in the simulation became similar to those obtained in the experiment as the system approached the steady state. Table 2 shows the composition of the gas exiting from the ATR and dummy stack in the steady state (positions A and C). The stimulated results differed from the experimental results by 7%–25%, which represents good agreement between the experimental and simulated values. However, a significant gap appears between the experiment and the simulation during early operation. It is due to a discrepancy in the initial heat loss and reaction speed at the ATR resulting from the simplified modeling.

These results indicate that this simulation method provides a guide for evaluating this BOP system. Hence, additional simulations were performed that modeled a real stack incorporated to the system,

A stack having a typical I–V curve and internal reforming was modeled instead of the dummy stack. Fuel utilization within the

stack was assumed to be in the range of 0.5–0.8. Four simulation cases were considered assuming the presence or absence of the internal reforming under the external heat transfer coefficient values; the simulation conditions are listed in Table 3.

Fig. 5 shows the estimated stack power, reformer efficiency, and system heat loss. The reformer efficiency of the ATR is defined as the ratio of the lower heating value of the produced H_2 and CO to that of the injected CH_4 within the ATR. The simulation estimated that the stack could produce power over a wide range (620–1600 W) in this BOP system, indicating that the stack power is significantly affected by the fuel utilization and internal reforming. The amount of available H_2 in the stack was relatively smaller without the internal reforming than with it. Less stack power was produced and more anode-off gas was consumed by the integrated heat exchanger and afterburner, increasing the temperature of the BOP system. Thus, the reformer efficiency improved slightly but the system heat loss increased because of the increased temperature of the gas. If the external heat transfer coefficient related to the environment was decreased to 50%, the system heat loss was reduced significantly, and the reformer efficiency was enhanced as well.

Table 4 shows the results of an energy analysis according to a fuel utilization of 0.7. The parasite loss, including the pump power loss and conversion loss of electricity, was assumed to be 20% with respect to the produced stack power. The net system efficiency varied significantly from 20% to 35% depending on the simulation conditions and it is essential to use the exhausted heat efficiently to enhance the system efficiency. Consequently, we estimate that this

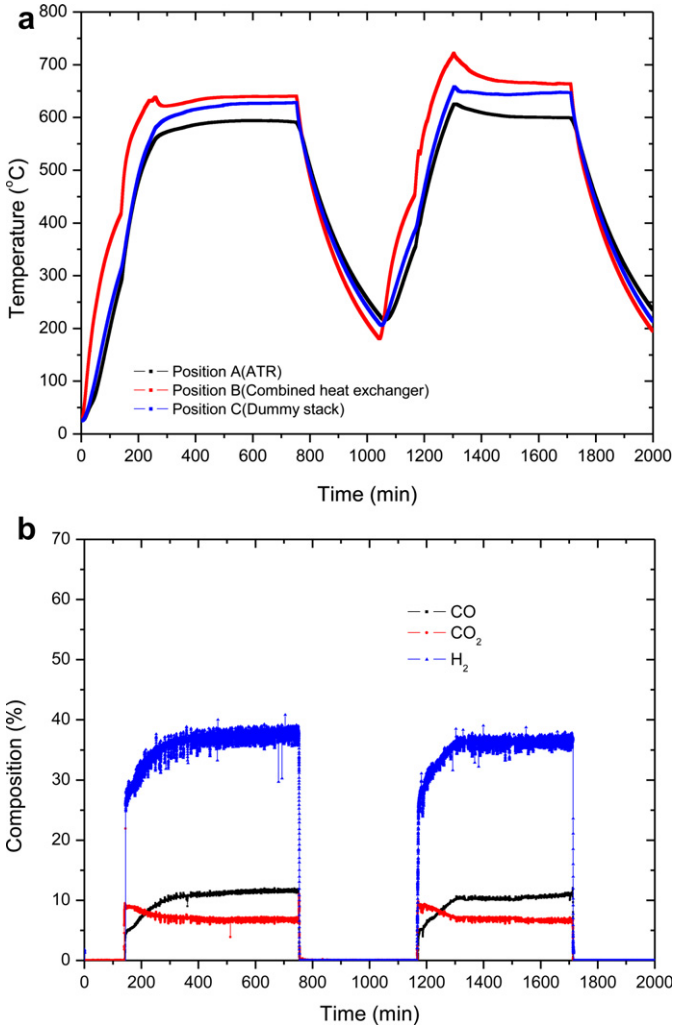

Fig. 3. History of temperature and reforming gas composition in SOFC BOP system. (a) Temperature of gas at each component. (b) Composition of reforming gas.

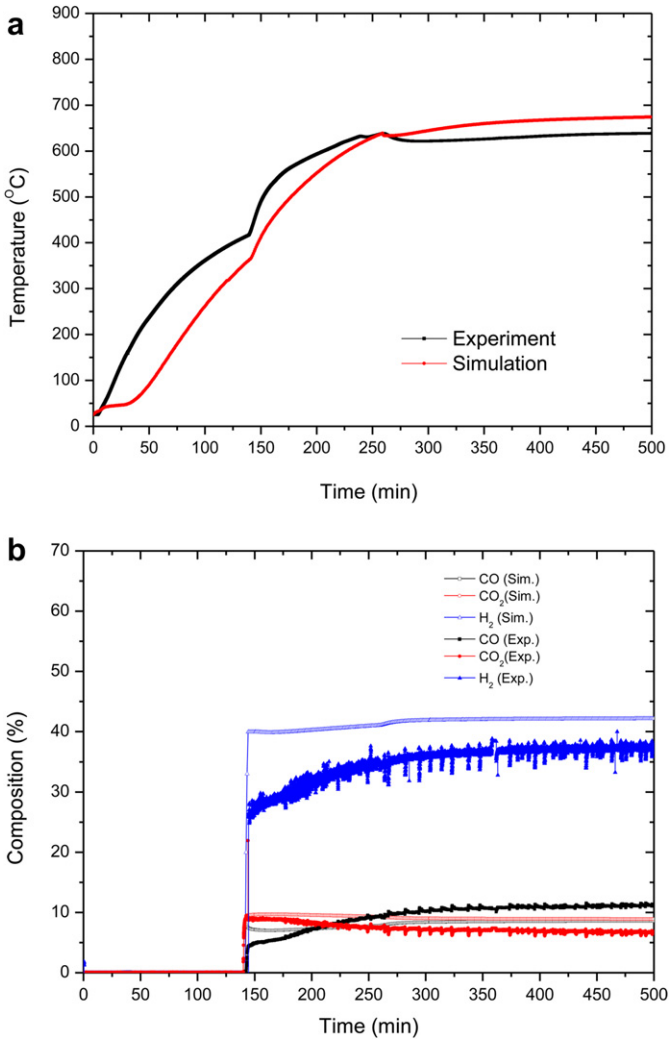

Fig. 4. Comparison of experimental and simulated data. (a) Temperature of cathode air from heat exchanger. (b) Composition of reforming gas.

Table 2
Variation in gas composition.

	Composition	Experiment (%)	Simulation (%)
ATR	H_2	36.4	41.9
	CO	11.0	8.4
	CO_2	6.5	8.9
Dummy stack	H_2	21.3	21.4
	CO	8.6	7.4
	CO_2	7.3	7.8

Table 3
Simulation cases.

	Internal reforming in stack	Reduction in external heat transfer coefficient
Case1	Yes	None
Case2	Yes	50%
Case3	No	None
Case4	No	50%

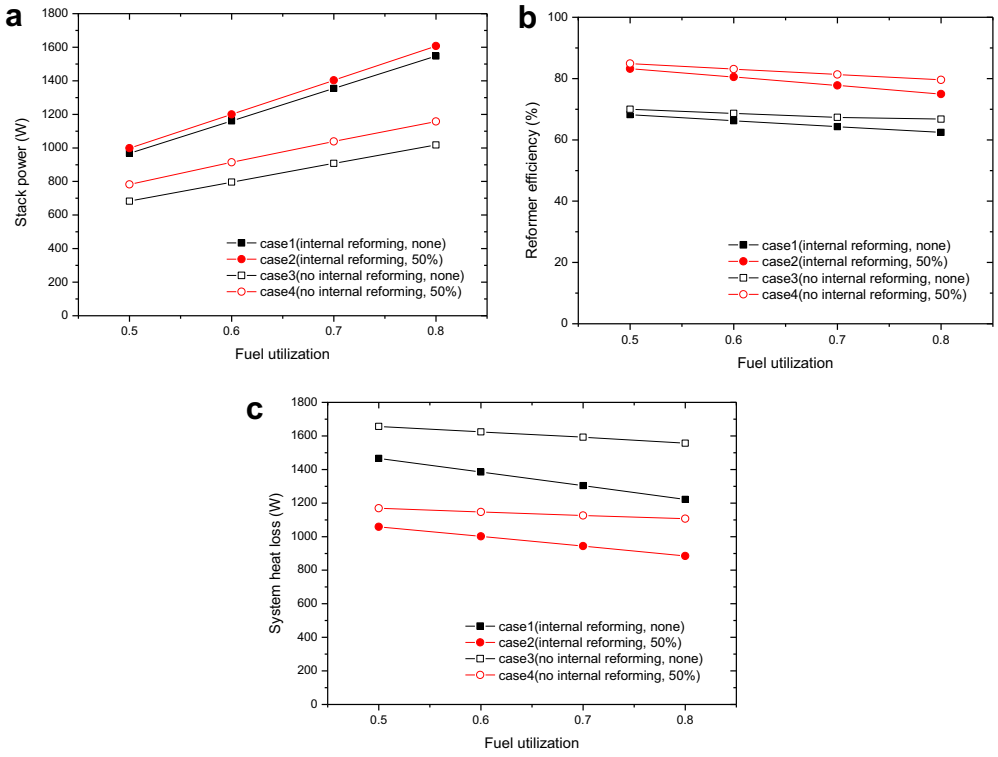

Fig. 5. Estimated results under different simulation conditions. (a) Stack power. (b) Reformer efficiency. (c) System heat loss.

Table 4
Simulated energy analysis.

	Case1	Case2	Case3	Case4
Input energy (W)	3777	3777	3777	3777
Stack power (W)	1354	1403	907	1038
Parasite loss (W)	271	281	181	208
System heat loss (W)	1304	944	1592	1126
Exhausted heat (W)	1119	1430	1278	1613
Net system efficiency (%)[a]	28.7	29.7	19.2	22.0
Combined system efficiency (%)[b]	58.3	67.6	53.0	64.7

[a] (stack power − parasite loss)/input energy × 100.
[b] (stack power − parasite loss + exhausted heat)/input energy × 100.

BOP system would be suitable for 1 kW SOFC operation if a stack with internal reforming is applied and the system heat loss is minimized.

5. Conclusions

A 1 kW SOFC BOP system was designed and operated; it included an ATR, a combined heat exchanger and afterburner, and dummy stack. A simulation using the simplified modeling was also conducted in order to evaluate the system.

The experimental results confirmed that the SOFC BOP system exhibited stable operation. Dynamic characteristics such as the variations in the temperature and the composition of gas were investigated experimentally and by simulation. Despite a discrepancy between experimental and simulated results early operation, good agreement was obtained as the system reached the steady state.

A simulation that incorporated a real stack predicted the variations in the BOP system's characteristics in terms of the fuel utilization, presence or absence of internal reforming, and external heat transfer coefficient. Consequently, we estimated that the BOP system would be suitable for 1 kW SOFC operation if a stack with internal reforming is applied and the system heat loss is minimized.

References

[1] J. Larminie, A. Dicks, Fuel Cell Systems Explained, second ed. Wiley, Chichester, 2003.
[2] Anon, Fuel Cell Handbook, seventh ed. NETL, Morgantown, 2004.
[3] P.K. Cheekatamarla, C.M. Finnerty, C.R. Robinson, S.M. Andrews, J. Power Sources 193 (2009) 797–803.
[4] J. Lawrence, M. Boltze, J. Power Sources 154 (2006) 479–488.
[5] N. Lu, Q. Li, X. Sun, M.A. Khaleel, J. Power Sources 161 (2006) 938–948.
[6] A. Salogni, P. Colonna, Appl. Therm. Eng. 30 (2010) 464–477.
[7] M. Pekesn, R. Peters, L. Blum, D. Stolten, Int. J. Hydrogen Energy 34 (2009) 6425–6436.
[8] M. Sorrentino, C. Pianese, Y. Guezennec, J. Power Sources 180 (2008) 380–392.
[9] D. Shin, S. Dong, S. Woo, Y. Song, Development of the Core Technology for Solid Oxide Fuel Cell and Stack Module Technology(II), KIER-A72412 (2007).
[10] Thermolib User Manual Release 4.2, EUtech Scientific Engineering, 2009.
[11] W.M. Kays, M.E. Crawford, Convective Heat and Mass Transfer, third ed. McGraw-Hill, New York, 1993.
[12] J. Park, S. Lee, S. Kim, J. Bae, J. Fuel Cell Sci. Technol. 7 (2010) 051018.